In Silico Identification of Phytochemical Inhibitors Against the S1 Dihydrofolate Reductase Variant of Staphylococcus Aureus: Overcoming Trimethoprim Resistance

By

Safuan Ahmed

22146035

A thesis submitted to the School of Pharmacy in partial fulfillment of the requirements for the degree of Bachelor of Pharmacy (B.Pharm. Hons.)

School of Pharmacy

BRAC University

May 2026

Declaration

It is hereby declared that

1. The thesis submitted is my own original work while completing my degree at BRAC University.
2. The thesis does not contain material previously published or written by a third party, except where this is appropriately cited through full and accurate referencing.
3. The thesis does not contain material which has been accepted, or submitted, for any other degree or diploma at a university or other institution.
4. I have acknowledged all main sources of help.

Student's Full Name & Signature:

Safuan Ahmed
22146035

Approval

The thesis titled "*In Silico* Identification of Novel Phytochemical Inhibitors Against the S1 Dihydrofolate Reductase Variant of Staphylococcus aureus: Overcoming Trimethoprim Resistance" submitted by Safuan Ahmed (ID: 22146035) of Spring, 2022 has been accepted as satisfactory in partial fulfillment of the requirement for the degree of Bachelor of Pharmacy

Examining Committee:

Supervisor:

Humair Bin Md. Omer, PhD
Associate Professor,
School of Pharmacy,
BRAC University

Approved By:

Chairperson:

Sharmind Neelotpol, PhD
Professor
School of Pharmacy
BRAC University

Dean

Professor Arshad Mahmud Chowdhury, PhD
Dean, School of Pharmacy
Pro Vice-Chancellor
Office of the Vice Chancellor
BRAC University

Ethics Statement:

This project did not involve any animal or human trials.

Abstract

This study addresses the critical challenge of trimethoprim (TMP) resistance in *Staphylococcus aureus* mediated by the plasmid encoded S1 DHFR variant. Using protein crystal structure (PDB ID: 2W9S), *in silico* molecular docking was performed to identify phytochemical inhibitors capable of overcoming the structural barriers of the S1 variant, such as a widened active site and M20 loop displacement. A library of phytochemicals from the Jahangirnagar University campus flora was screened against the mutant enzyme. Virtual screening results identified Rutin (−9.5 kcal/mol), Neferine (−9.2 kcal/mol), and Rosmarinic acid (−8.95 kcal/mol) as top candidates with better binding affinities than the standard Trimethoprim (−7.8 kcal/mol). These compounds demonstrate high binding affinity and stability, suggesting their potential to bridge the altered active site of the S1 variant. These early findings provide a molecular docking approach for potentially developing next-generation "resistance-breaking" antibiotics to combat multidrug-resistant methicillin-resistant staphylococcus aureus (MRSA).

Keywords: Staphylococcus aureus, S1 DHFR, Molecular docking, Phytochemicals, Trimethoprim

Acknowledgement

I want to start by conveying my heartfelt thanks to the Almighty for providing me with the strength, patience, and determination to finish this project. I extend my sincere gratitude to my supervisor, Dr. Humair Bin Md Omer, Associate Professor, School of Pharmacy, BRAC University, whose consistent support, thoughtful advice, and steadfast motivation were essential throughout this work.

I extend my heartfelt appreciation to Dr. Sharmind Neelotpol, Professor and Chairperson, School of Pharmacy, BRAC University, for creating a nurturing academic atmosphere throughout my undergraduate education.

I want to convey my heartfelt thanks to my parents, whose unwavering love, support, and faith in my potential.

I express our gratitude to my friends who helped or supported me directly or indirectly, in finishing this project.

Table of Contents

List of Tables:

List of Figures:

List of Acronyms

TMP — Trimethoprim.

DHFR — Dihydrofolate reductase.

MRSA — Methicillin-resistant *Staphylococcus aureus*.

MSSA — Methicillin-susceptible *Staphylococcus aureus*.

VISA — Vancomycin-intermediate *Staphylococcus aureus*.

VRSA — Vancomycin-resistant *Staphylococcus aureus*.

CoNS — Coagulase-negative staphylococci.

PBP — Penicillin-binding proteins.

PBP2a — Altered penicillin-binding protein encoded by *mecA*.

TSS — Toxic shock syndrome.

TSST-1 — Toxic shock syndrome toxin-1.

PVL — Panton-Valentine leukocidin.

CPK — Creatinine phosphokinase.

MAO — Monoamine oxidase.

ADMET — Absorption, distribution, metabolism, excretion, and toxicity.

SAR — Structure-activity relationship.

MD — Molecular dynamics.

PDB — Protein Data Bank.

S1 — The plasmid-encoded DHFR variant discussed in the thesis.

GOL — Glycerol.

NDP — NADPH.

TOP — Trimethoprim

Chapter: 1

Introduction to Staphylococcus

Staphylococcus is a genus of Gram-positive bacteria that appear spherical (cocci) under a microscope, often clustering together like grapes. The name comes from the Ancient Greek words for "bunch of grapes" (staphyle) and "berry" (kokkos) (Licitra, 2013). While many species of Staphylococcus are harmless and live on the skin or mucous membranes of humans and animals, some are significant pathogens. The most well-known and dangerous species is *Staphylococcus aureus*, often called "golden staph" (Encyclopaedia Britannica, 2025).

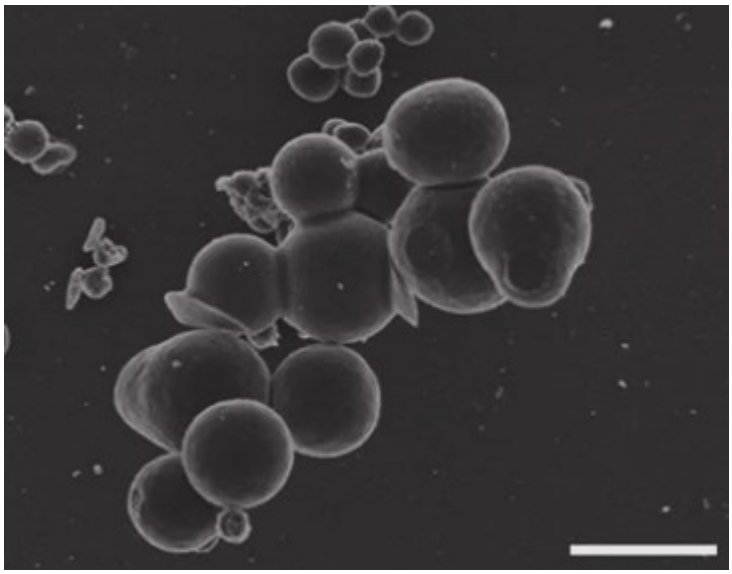

Figure 1: Scanning electron micrograph of *S. aureus* (Bozdogan et al., 2012)

At least 30 species of Staphylococcus are recognized. Though most are harmless commensals, a few are important human or animal pathogens. The medically relevant species are generally divided into two main categories, based on the coagulase test that checks for the presence of the enzyme coagulase.

Coagulase-positive staphylococci:

Staphylococcus aureus is the most significant species in this group and the most dangerous human pathogen of the genus. A few other coagulase-positive species exist, like those found in animals, but they occur much less frequently in human disease (Foster, 2025).

Coagulase-negative staphylococci (CoNS):

This group contains most Staphylococcus species. Once thought to be harmless, many are now recognized as opportunistic pathogens, particularly in patients with weakened immune systems or those with medical devices.

The most important CoNS species include:

Staphylococcus epidermidis: This is the most frequent CoNS pathogen linked to infections from implanted medical devices like catheters and artificial joints.

Staphylococcus saprophyticus: This species is a common cause of urinary tract infections, especially in young women.

Staphylococcus lugdunensis: This species can cause serious infections that sometimes resemble those caused by *S. aureus* (UK Standards for Microbiology Investigations, 2020).

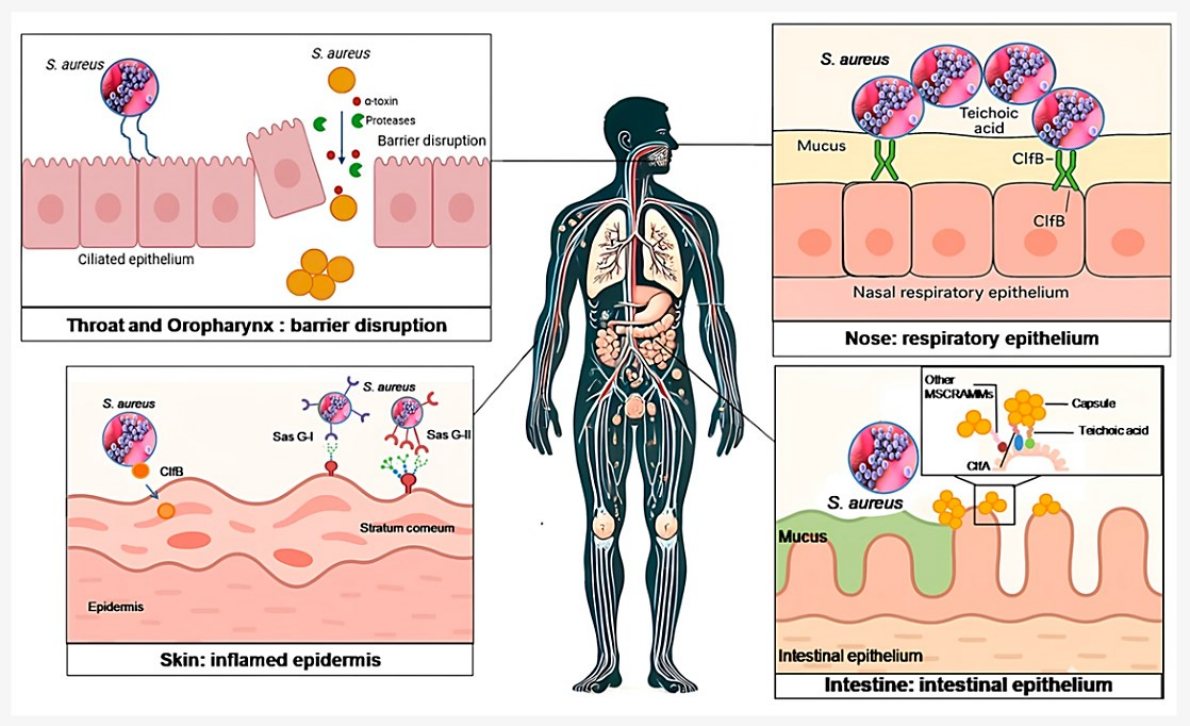

Figure 2: Host–Epithelium Interaction with *S. aureus* (Touaitia et al., 2025)

1.1 Key characteristics

Gram-positive: They maintain the crystal violet stain used in the Gram stain procedure because of their thick peptidoglycan cell walls.

Morphology: These are spherical bacteria (cocci) that usually arrange themselves in grape-like clusters.

Facultative anaerobes: These can grow with or without oxygen.

Catalase-positive: They produce the enzyme catalase, distinguishing them from other bacteria such as streptococci.

Salt resistance: They can resist high salt concentrations, a property utilized in some laboratory identification media (Foster, 2025).

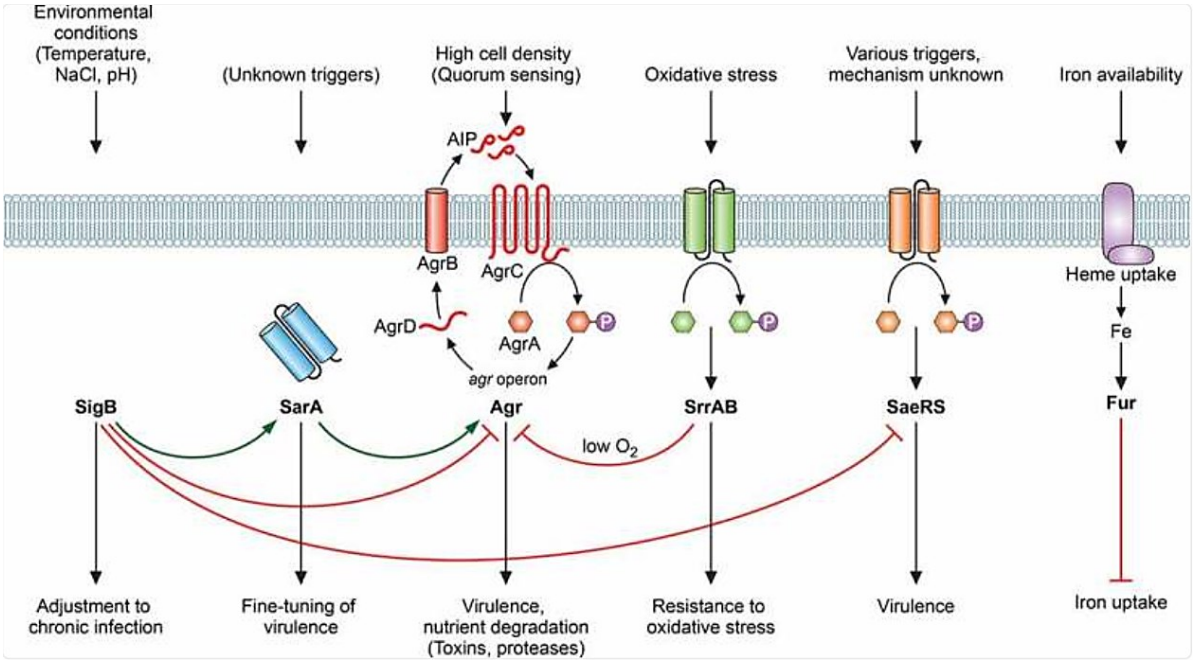

Figure 3: Regulation of virulence in *S. aureus.* (Cheung, Bae, & Otto, 2021)

1.2 Origins in human and animal hosts

For many of the species of Staphylococcus, their origins are intimately related with their role as colonizers of human and animal hosts:

Staphylococcus aureus: Genetic studies indicate that the modern lineage of *S. aureus* has a long evolutionary history of adaptation to its mammalian hosts. Comparative genomic studies on a particular lineage, for instance, have tracked the origins of Staphylococcus aureus ST45 back to northwestern Europe around 500 years ago (Effelsberg et al., 2021).

Figure 5 denotes Countries where isolates were obtained from are shaded in light gray. Transmissions are indicated with arrows and colored according to the three major phylogenetic groups that were identified. Acquisition of agr and cap type is highlighted. The dating of transmission (95% HPD interval) as calculated by BEAST is given. Major lineages circulating to date are marked with blue, circular arrows, and the respective labels while figure 4 denotes global distribution of *S. aureus* ST45. Countries with CC45 isolates reported in the

literature (as of February 2019) are colored in blue. The darker shade marks countries with ST45 isolates that were available for this study

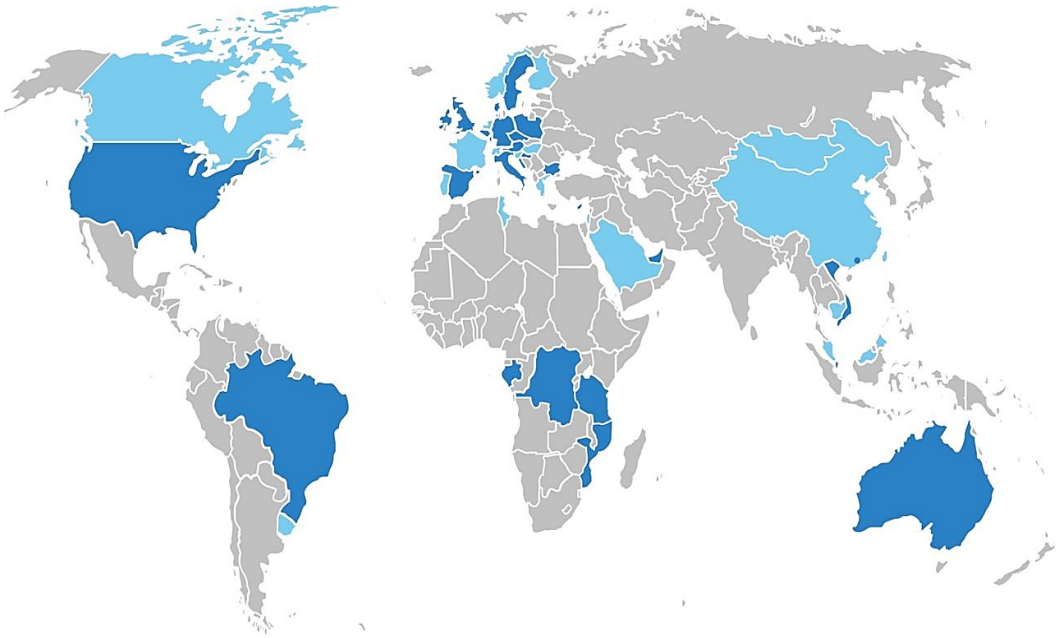

Figure 4: Global distribution of *S. aureus* ST45. (Effelsberg et al., 2021)

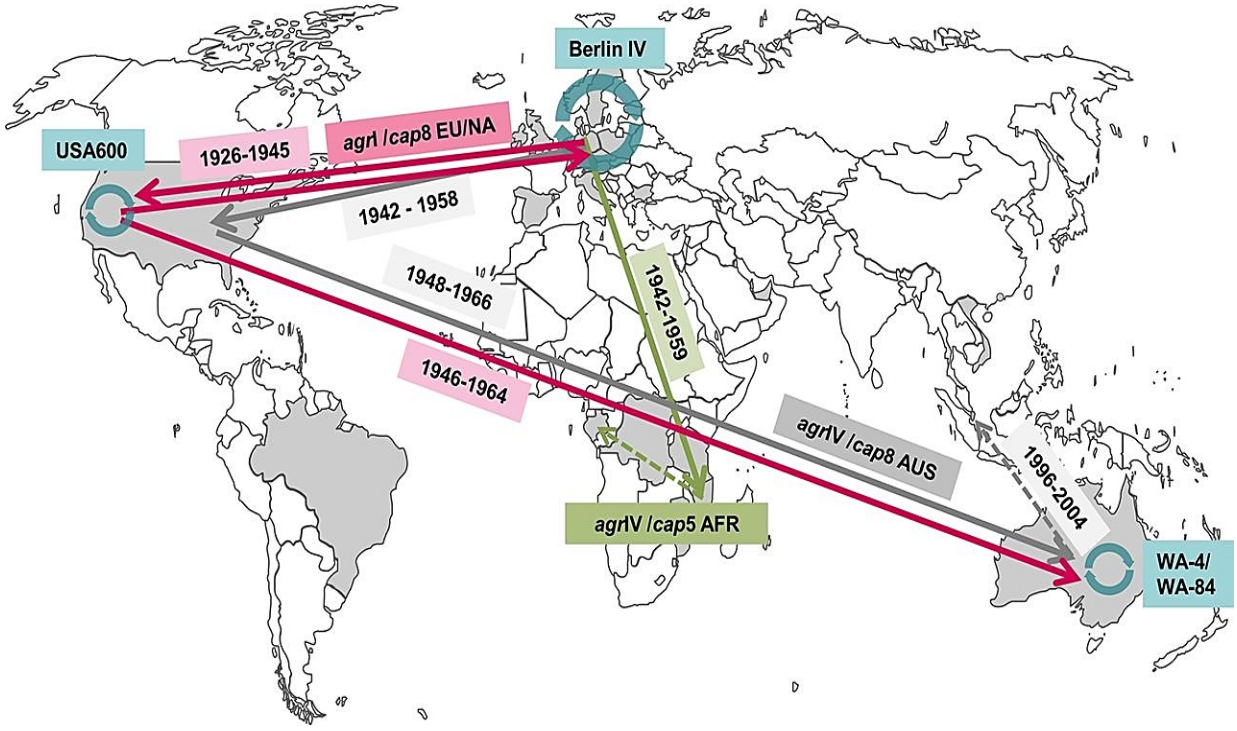

Figure 5: Map of major transmission events (Effelsberg et al., 2021)

1.3 Evolution and antibiotic resistance

One major aspect of the evolution of Staphylococcus is its rapid adaptation and acquisition of antibiotic resistance. This is clearly not the result of a single origin but rather from a series of events over time due to human activity.

Early penicillin resistance: The first wave of resistance began shortly after the introduction of penicillin in the 1940s. In the late 1940s, penicillin resistance became widespread in *S. aureus* populations due to a penicillin-inactivating enzyme produced by the bacteria.

Methicillin-resistant *S. aureus* (MRSA): The first MRSA strains showed up in hospitals shortly after the introduction of the new antibiotic methicillin in the early 1960s. MRSA's resistance is due to the acquisition of the mecA gene which is a mobile genetic element that can be transferred between different staph strains.

Vancomycin resistance: More recently, vancomycin-intermediate *S. aureus* (VISA) and vancomycin-resistant *S. aureus* (VRSA) have emerged, primarily in health care settings, due to vancomycin-related selective pressures (Chambers & DeLeo, 2009).

1.4 Infection process

Staphylococcal infection is a multistep process. It begins when bacteria colonize the body. They then use their virulence factors to cause damage that ranges from localized skin infections to severe systemic illnesses.

Stage 1: Colonization

The process starts with Staphylococcus aureus colonizing the body. About 30% of people carry these bacteria harmlessly on their skin or in their noses.

Adhesion: Staph bacteria have proteins called adhesins on their surface. These help them stick to the host's tissues.

Establishment: Once attached, the bacteria start to take over specific areas of the body, such as the nasal passages or moist areas of skin.

Stage 2: Exposure and invasion

Infection often occurs when bacteria have the opportunity to penetrate further into the body.

Skin breach: When the skin is damaged by a cut, scrape, surgical cut, or insertion of a medical device, bacteria can penetrate the deeper tissues.

Initial immune reaction: The immune system deploys immune cells, such as neutrophils, to combat the bacteria. Nevertheless, staph employs defenses against these assaults, such as surface proteins that assist it in evading detection and elimination by immune cells.

Localized infection: The bacteria start to proliferate and utilize their virulence factors to establish a localized infection.

Abscess formation: Staph produces an enzyme called coagulase that causes blood plasma to clot. This leaves the bacteria surrounded by a fibrin capsule, which protects the abscess from immune cells and antibiotics.

Tissue destruction: Toxins such as alpha-toxin and Panton-Valentine leukocidin (PVL) kill white blood cells and lead to the death of nearby tissue.

Stage 3: Systemic infection

If the bacteria or their toxins manage to overcome local defenses, a general body infection can develop into a more serious disease.

Bloodstream entry: The infection can lead to bacteremia, either through a persistent wound or an abscess, and spread to the other parts of the body.

Organ infection: Once in the bloodstream, staph can reach other organs and tissues, causing:

Endocarditis: Infection of the inner lining of the heart and the valves.

Osteomyelitis: Infection of the bones or joints.

Pneumonia: Infection of the lungs.

Biofilm formation: If the infection is near a medical implant, staph can form a biofilm that is very resistant to treatment and may require the removal of the device.

Stage 4: Extensive damage

In extreme instances, staph may emit potent toxins into the blood, leading to significant harm.

TSS: Certain strains produce superantigens such as TSST-1. These toxins provoke a significant, unregulated immune reaction, resulting in the release of inflammatory substances that may harm organs and induce fever and rash.

Sepsis and septic shock: An excessive immune reaction can lead to sepsis. This can result in septic shock, characterized by a significant decline in blood pressure and the malfunction of several organs.

Stage 5: Resolution or continued damage

The ultimate result relies on the infection's severity and the effectiveness of the treatment.

Recovery: Through successful therapy, the immune system eliminates the bacteria, allowing the body to start mending harmed tissues.

Long-term Consequences after Sepsis: Individuals who survive severe systemic infections may face ongoing problems such as muscle weakness, sleep disturbances, fatigue, and possibly hallucinations.

Persistent infection: If a biofilm develops or if bacteria are not entirely eradicated, the infection may turn chronic (Liu, Garrett, Hong, & Zhang, 2024).

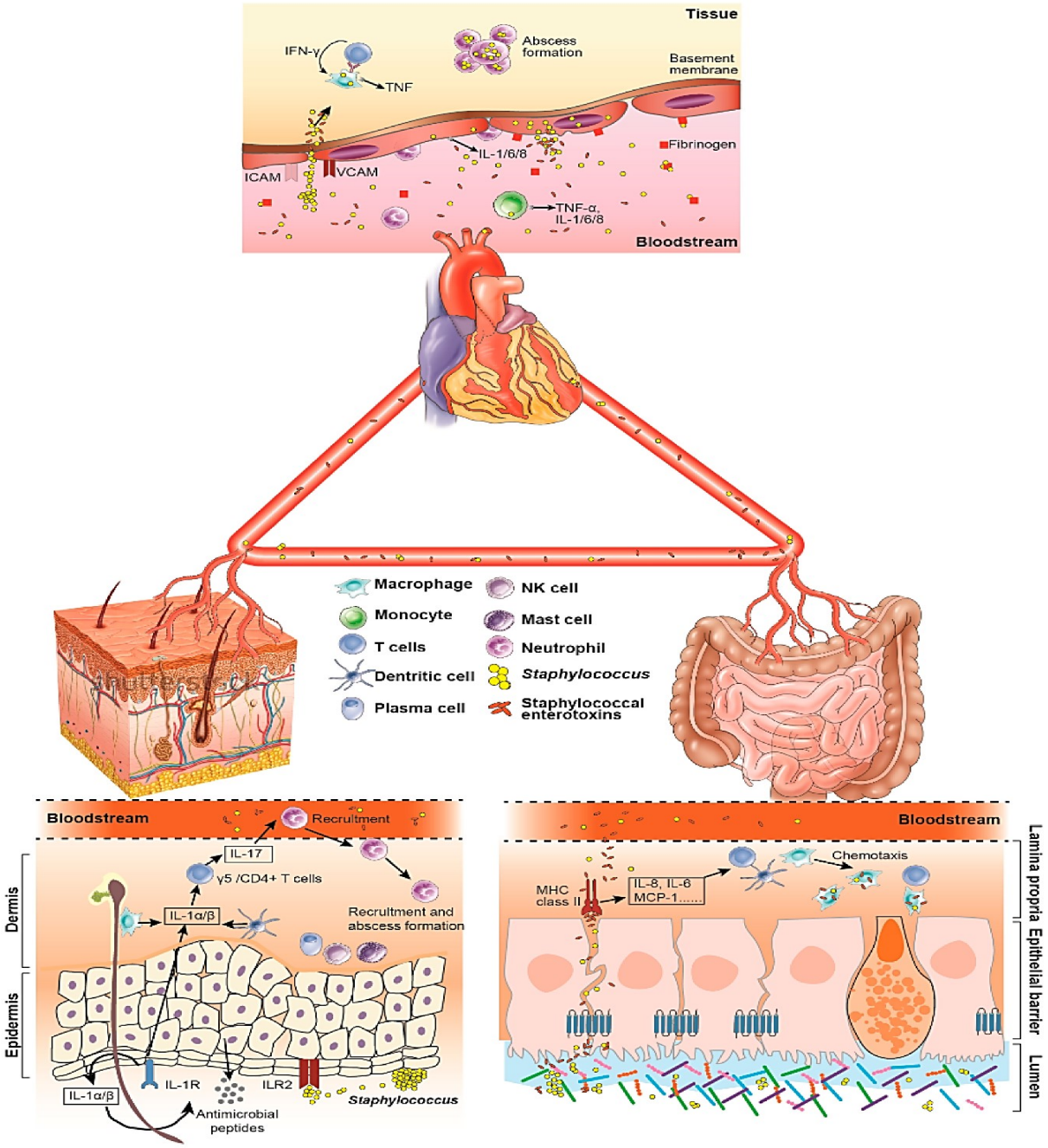

Figure 6: Systemic inflammatory crosstalk between the skin and the gut during a Staphylococcus aureus infection, showing how immune cells and cytokines circulate through the bloodstream to coordinate barrier defenses and abscess formation (Liu, Garrett, Hong, & Zhang, 2024)

1.5 Global prevalence

According to Hasanpour et al., (2023) the prevalence of Staphylococcus aureus varies widely around the world. This variation depends on the setting, such as healthcare or community, the population studied, and the specific strain like Methicillin-resistant *S. aureus* (MRSA).

Asymptomatic carriage: About 30% of the human population carries *S. aureus* without showing symptoms. It usually colonizes the nasal passages. The percentage of people carrying MRSA is much lower, estimated at around 1.3% in the general community.

Infections: *S. aureus* is a leading cause of infections globally. These include skin and soft tissue infections, bacteremia (bloodstream infection), infective endocarditis, and pneumonia.

Healthcare settings: MRSA is especially problematic in healthcare settings, where colonization and infection rates are much higher than in the community. In elders, a meta-analysis conducted in 2023 revealed a worldwide pooled MRSA prevalence of almost 15%.

Regional differences: Rates of prevalence vary by area. Historically, Europe has experienced lower MRSA rates compared to North America, though this differs significantly among countries. Increased antibiotic usage and variations in infection control measures might account for these discrepancies.

1.6 Prevalence in Bangladesh

Research from Bangladesh by Tania et al., (2023) highlights a major issue with Staphylococcus infections, especially stubborn antibiotic resistance to drugs like methicillin. A 2013 review of studies spanning 2000 to 2013 showed MRSA isolation rates among culture samples swinging wildly from 4.8% to as high as 78.7%.

Recent work in hospitals backs this up, with MRSA turning up in 32% to 72% of clinical samples according to a 2023 study. That same year, another study on hospitalized patients

found *S. aureus* in 21.63% of clinical specimens, and these bugs were notably resistant to everyday antibiotics like azithromycin and erythromycin.

Even healthcare workers aren't spared as a 2022 study in a Dhaka neonatal ICU found 18.4% of healthcare workers and caregivers carrying *S. aureus* in their noses, though luckily, none were MRSA in that group. However, a different 2023 study on healthcare workers in Jeshore reported an overall MRSA prevalence of 3.53%.

Antibiotic resistance: In addition to methicillin resistance, multi-drug resistance (MDR) is a significant concern in Bangladesh. National surveillance of antimicrobial resistance found that 8% of tested isolates from 2017 to 2022 showed possible pan-drug resistance. A 2021 study of human and animal samples highlighted high rates of antibiotic resistance among *S. aureus* isolates, particularly against penicillin.

Environmental and animal reservoirs: Concerns about MDR-MRSA extend beyond human infections. A December 2024 study in Bangladesh found MDR-MRSA in livestock, especially goats, which indicates a potential public health risk from animal sources.

1.7 Rationale for choosing 2W9S:

The study conducted by Heaslet et al. (2009) provides a high-resolution analysis of how Staphylococcus aureus becomes resistant to the antibiotic trimethoprim (TMP). By comparing the chromosomal wild-type enzyme with the plasmid-encoded S1 variant, the researchers identified the specific physical changes that prevent the drug from functioning.

The researchers deposited several structures into the Protein Data Bank, but 2W9S is the primary focus for drug discovery. It represents the S1 DHFR ternary complex which is the resistant enzyme bound to both the drug (TMP) and its necessary cofactor (NADPH) at a resolution of 1.8 Å.

This specific structure is used because it captures the exact molecular interface where the drug fails to bind effectively. By observing the S1 variant in its active state, scientists can identify the geometric differences between the resistant and non-resistant versions of the enzyme.

The 2W9S structure reveals that the S1 variant undergoes several coordinated changes in its active site. These alterations reduce the stability of the drug-protein complex:

- **M20 Loop Displacement**: In the wild-type enzyme, the M20 loop shifts into a closed conformation to surround the drug. In the S1 variant (2W9S), this loop remains in an open or misaligned position, failing to secure the TMP molecule.
- **Active Site Widening**: Changes in the betaF-betaG protein sheets cause the binding pocket to widen. This increase in volume reduces the proximity required for strong molecular interactions.
- **Phe92 Rotation**: The residue Phenylalanine-92 rotates away from the phenyl ring of the TMP molecule. This movement eliminates the pi-stacking interactions that normally provide significant binding energy.
- **Helix alpha5 Shift**: A lateral movement of approximately 2 Å in the alpha5 helix disrupts the hydrogen bonds that typically connect the protein to the drug's aminopyrimidine group.
- **Loss of Cooperativity**: In the wild-type, the presence of the NADPH cofactor increases the enzyme's affinity for TMP. The S1 variant lacks this synergy, further weakening the drug's attachment.

Chapter 2

Methodology

2.1 Protein preparation

To prepare the receptor for molecular docking, using the 2W9S structure, the following protocol is used. These steps ensure the removal of crystallographic artifacts and the proper parameterization of the protein for the AutoDock Vina environment.

2.1.1 Phase 1: Structure Cleaning & Preparation (Discovery Studio)

This phase involves removing non-essential molecules and standardizing the polypeptide chains.

1. Acquisition: Download the protein from the RCSB PDB database in the Legacy PDB format.

2. Initialization: Open the `.pdb` file in Discovery Studio.

3. Visualization: Navigate to `View` → `Hierarchy` to open the selection tree.

4. Solvent Removal: Click on Water in the Hierarchy window (molecules will turn yellow). Navigate to `Edit` → `Delete`. Manually inspect the structure for other crystallographic solvents (e.g., Glycerol, Sulfate). Select these and delete them.

5. Chain Standardization:

I. Expand the polypeptide chains (Chain A, B, C, etc.) by clicking the + sign.

II. Evaluate if chains are duplicates. If Chain B is a redundant copy of Chain A, delete the redundant chain.

6. Intermediate Save: Save the modified file as `protein-modified.pdb`. Ensure the "Save as type" is set to Protein Data Bank Files.

2.1.2 Phase 2: Binding Site Definition & Coordinate Extraction

In this stage, we define the search space (grid box) based on the co-crystallized ligand position.

7. Identify Ligand: Select the co-crystallized ligand from the Hierarchy window.

8. Define Site: Navigate to `Receptor-Ligand Interactions` → `Define and Edit Binding Site` → `From Current Selection`.

9. Extract Coordinates: A red sphere (`sbd_site_sphere`) will appear. Right-click it and select `Attributes of sbd_site_sphere`. Note the X, Y, and Z coordinates and copy these values into your configuration file.

10. Final Clean: Exit the dialog, delete both the `sbd_site_sphere` and the co-crystallized ligand.

11. Save Receptor: Save the file as `protein.pdb` (ensure the format remains Protein Data Bank Files).

2.1.3 Phase 3: Parameterization & PDBQT Conversion (AutoDock Tools)

This phase prepares the protein for the forcefield by adding charges and atom types.

12. Load Molecule: Open `protein.pdb` in AutoDock Tools via `File` → `Read Molecule`.

13. Selection: Click the small box in the GUI to select all atoms.

14. Atom Repair:

I. Go to `Edit` → `Misc` → `Check for Missing Atoms` → `Select all residues` → `Dismiss`.

II. Navigate to `Edit` → `Misc` → `Repair Missing Atoms`. Click `Save as 2 sets` when prompted.

15. Hydrogen & Charge Assignment:

I. Add Hydrogens: `Edit` → `Hydrogens` → `Add` → `Polar Only`.

II. Assign Charges: `Edit` → `Charges` → `Add Kollman Charges`.

III. Balance Charges: `Edit` → `Charges` → `Check Totals on Residues`. Select `Spread charge deficit over all atoms`.

Verification: Re-check totals until the message "No residues with non-integral charges found" appears.

16. Atom Typing: Navigate to `Edit` → `Atoms` → `Assign AD4 Type`.

17. Define Macromolecule: Go to `Grid` → `Macromolecule` → `Choose` → Select your protein.

18. Final Export: Save the final structure as `protein.pdbqt`. Verify that the file extension is strictly `.pdbqt`.

2.2 Phytochemical selection

I have selected Vegetables from Jahangirnagar University campus flora, their paper is titled: **Floristic composition of Jahangirnagar University Campus - A semi-natural area of Bangladesh** (Khan, Sultana, Hossain, Shetu, & Rahim, 2021).

Below is the list of selected vegetables categorized by their local names, scientific names, and English common names:

Table 1: list of vegetables categorized by their local names, scientific names, and English common names

Local Name (Bangla)	Scientific Name	English Common Name
Sada shapla	*Nymphaea pubescens*	White Water Lily
Lal shapla	*Nymphaea rubra*	Red Water Lily
Kantanotey	*Amaranthus spinosus*	Spiny Amaranth
Boronunia	*Portulaca oleracea*	Purslane
Pui shak	*Basella alba*	Malabar Spinach
Dherosh	*Abelmoschus esculentus*	Okra
Pat	*Corchorus capsularis*	Jute
Pepe	*Carica papaya*	Papaya
Chalkumra	*Benincasa hispida*	Wax Gourd
Telakucha	*Coccinia grandis*	Ivy Gourd
Kakur	*Cucumis melo*	Melon

Khira	*Cucumis sativus*	Cucumber
Kumra	*Cucurbita maxima*	Pumpkin
Lao	*Lagenaria siceraria*	Bottle Gourd
Jhinga	*Luffa acutangula*	Ridge Gourd
Dhundal	*Luffa cylindrica*	Sponge Gourd
Korolla	*Momordica charantia*	Bitter Gourd
Potol	*Trichosanthes dioica*	Pointed Gourd
Chichinga	*Trichosanthes cucumerina*	Snake Gourd
Shajna	*Moringa oleifera*	Drumstick
Sarisha	*Brassica juncea*	Mustard
Dhonia	*Coriandrum sativum*	Coriander
Kalmishak	*Ipomoea aquatica*	Water Spinach
Begun	*Solanum melongena*	Eggplant
Man kachu	*Alocasia macrorrhizos*	Giant Taro
Jangli kachu	*Colocasia esculenta*	Taro
Kach kola	*Musa paradisiaca*	Green Banana (Plantain)
Chupri alu	*Dioscorea alata*	Purple Yam

Though most phytochemicals were not found for all the samples, the following looked the most promising and were selected for further steps; all of these were downloaded from PubChem https://pubchem.ncbi.nlm.nih.gov/

Table 2: Phytochemicals that were used in testing

No.	Compound Identifier
1	1-octanol-Conformer3D_COMPOUND_CID_957
2	2,3,5,6-tetrafluoroanisole-Conformer3D_COMPOUND_CID_75351
3	2-decen-1-ol_Conformer3D_COMPOUND_CID_87630
4	4-Acetoxy-2-azetidinone-Conformer3D_COMPOUND_CID_119981
5	4-Hydroxy-4-methyl-2-pentanone-Conformer3D_COMPOUND_CID_31256
6	4-Hydroxy-benzoic-acid-Conformer3D_COMPOUND_CID_135
7	6-Methyl-5-hepten-2-one-Conformer3D_COMPOUND_CID_9862
8	Alloaromadendrene-Conformer3D_COMPOUND_CID_10899740
9	Alpha-tocopherol-Conformer3D_COMPOUND_CID_86472
10	Anthocyanins-Conformer3D_COMPOUND_CID_145858
11	Beta-tocopherol-Conformer3D_COMPOUND_CID_6857447
12	C17H34O2-Conformer3D_COMPOUND_CID_8042
13	C4H8O3-Conformer3D_COMPOUND_CID_10413
14	C5H7O3N-Conformer3D_COMPOUND_CID_7405
15	C7H14O-Conformer3D_COMPOUND_CID_8051
16	C8h8o-Conformer3D_COMPOUND_CID_62453

17	C8H8O2-Conformer3D_COMPOUND_CID_13131455
18	Caffeic-acid-Conformer3D_COMPOUND_CID_689043
19	Camphene-Conformer3D_COMPOUND_CID_6616
20	Camphor-Conformer3D_COMPOUND_CID_2537
21	Carvone-Conformer3D_COMPOUND_CID_7439
22	Catechin-Conformer3D_COMPOUND_CID_9064
23	Chlorogenic-acid-Conformer3D_COMPOUND_CID_1794427
24	Cis-13-OctadecenoicacidConformer3D_COMPOUND_CID_5312441
25	Conformer3D_COMPOUND_CID_5280804
26	Cucurbitin-Conformer3D_COMPOUND_CID_442634
27	Cyclodecane-Conformer3D_COMPOUND_CID_9267
28	Decanal-Conformer3D_COMPOUND_CID_8175
29	Dodecanal-Conformer3D_COMPOUND_CID_8194
30	(E)-Anethole-Conformer3D_COMPOUND_CID_637563
31	Ellagic-acid-Conformer3D_COMPOUND_CID_5281855
32	Eugenol-Conformer3D_COMPOUND_CID_3314
33	Exo-fenchyl-acetate-Conformer3D_COMPOUND_CID_6430689
34	Ferulic-acid-Conformer3D_COMPOUND_CID_445858
35	Gallic-acid-Conformer3D_COMPOUND_CID_370
36	Geraniol-Conformer3D_COMPOUND_CID_637566
37	Geranyl-acetate-Conformer3D_COMPOUND_CID_1549026

38	Hexadecanoic-acid-Conformer3D_COMPOUND_CID_985
39	Kaempferol-3-O-glucoside-Conformer3D_COMPOUND_CID_24211971
40	Limonene-Conformer3D_COMPOUND_CID_22311
41	Linalool-Conformer3D_COMPOUND_CID_6549
42	Linalyl-acetate-Conformer3D_COMPOUND_CID_8294
43	Lutein-Conformer3D_COMPOUND_CID_5281243
44	Menthol-Conformer3D_COMPOUND_CID_1254
45	Myrcene-Conformer3D_COMPOUND_CID_31253
46	Myricetin-Conformer3D_COMPOUND_CID_5281672
47	N-Decanoic-acid-Conformer3D_COMPOUND_CID_2969
48	N-dodecane-Conformer3D_COMPOUND_CID_8182
49	Neferine-Conformer3D_COMPOUND_CID_159654
50	Neochlorogenic-acid-Conformer3D_COMPOUND_CID_5280633
51	N-tetradecane-Conformer3D_COMPOUND_CID_12389
52	N-tridecane-Conformer3D_COMPOUND_CID_12388
53	Nuciferine-Conformer3D_COMPOUND_CID_10146
54	N-Undecane-Conformer3D_COMPOUND_CID_14257
55	Nymphayol-Conformer3D_COMPOUND_CID_44591829
56	P-coumaric-acid-Conformer3D_COMPOUND_CID_637542
57	P-cymene-Conformer3D_COMPOUND_CID_7463
58	Petroselinic-acid-Conformer3D_COMPOUND_CID_5281125

59	Protocatechuic-acid-Conformer3D_COMPOUND_CID_72
60	Quercetin-Conformer3D_COMPOUND_CID_5280343
61	Rosmarinic-acid-Conformer3D_COMPOUND_CID_5281792
62	Rutin-Conformer3D_COMPOUND_CID_5280805
63	Sinapic-acid-Conformer3D_COMPOUND_CID_10743
64	Terpinen-4-ol-Conformer3D_COMPOUND_CID_11230
65	Trans-2-decenal-Conformer3D_COMPOUND_CID_5283345
66	Trigonelline-Conformer3D_COMPOUND_CID_5570
67	Vanillic-acid-Conformer3D_COMPOUND_CID_8468
68	Violaxanthin-Conformer3D_COMPOUND_CID_448438
69	Zeaxanthin-Conformer3D_COMPOUND_CID_5280899

2.3 Virtual Screening and Molecular Docking

To perform a high-throughput virtual screening using AutoDock Vina, this structured protocol is followed. This workflow ensures that your ligands are properly protonated, converted, and docked against the prepared receptor (protein.pdbqt)

2.3.1 Phase 1: Ligand Acquisition & 3D Preparation

Proper geometric and ionization states are critical for accurate docking results.

1. Download Structures: Obtain 3D ligand structures in SDF format from databases like PubChem.
2. Ensure 3D Conformation: If 3D structures are unavailable, retrieve them from RCSB PDB or manually convert 2D structures to 3D using Avogadro.

3. Protonation (pH 7.4):
    - Avogadro: Open the structure → Build → Add Hydrogens for pH → Set pH = 7.4.
4. Quality Control: Save the files in SDF format. Open them in Avogadro to visually verify that the 3D geometry and hydrogens appear correct.
5. Storage: Store all prepared SDF files in a single dedicated folder.

2.3.2 Phase 2: File Conversion & Batch Preparation

Before docking, ligands must be converted to the PDBQT format, which contains the partial charges and atom types required by Vina.

6. Format Conversion: Convert all sdf ligand files into pdbqt using OpenBabel
7. Validation: Visually inspect the newly created .pdbqt files in Avogadro to ensure no errors occurred during conversion.

2.3.3 Phase 3: Docking

Run the docking of every ligand in the list and compile the results into an excel file. The parameters for docking are x = 17.288917, y = 4.247917 and z = 38.249625 for binding pockets and the box length is 20.

Chapter: 3

Commonly used drugs for treating Staphylococcus infection

The choice of antibiotic depends on whether the strain is Methicillin-susceptible Staphylococcus aureus (MSSA) or Methicillin-resistant *S. aureus* (MRSA), and the severity of the said infection.

Table 3: Strain of Staphylococcus

Infection Type	First-Line Antibiotics	Alternatives for Allergy or Resistance
MSSA	Nafcillin, Oxacillin, Dicloxacillin, Cefazolin	Clindamycin, Vancomycin
MRSA	Vancomycin, Linezolid, Daptomycin	Clindamycin, Trimethoprim/sulfamethoxazole, Doxycycline, Dalbavancin
Minor Skin Infections	Topical mupirocin or retapamulin; Oral clindamycin or trimethoprim/sulfamethoxazole (for suspected MRSA)	
Biofilm Infections	Often combination therapy, e.g., rifampin plus another agent (vancomycin or daptomycin), as rifampin has high activity against biofilms	

3.1 Mechanisms of Action

Beta-lactam antibiotics (e.g., Methicillin, Nafcillin, Oxacillin, Cefazolin): These drugs block the synthesis of the bacterial cell wall by binding to penicillin-binding proteins (PBPs). PBPs are necessary for linking peptidoglycan. This action weakens the cell wall, leading to bacterial lysis and death. MRSA strains have a modified low-affinity PBP (PBP2a) encoded by the

mecA gene. This modification prevents beta-lactam antibiotics from binding effectively, resulting in resistance (Shao et al., 2025).

Vancomycin and other Glycopeptides (e.g., Teicoplanin, Dalbavancin, Oritavancin): These antibiotics also block bacterial cell wall synthesis. They bind to the D-alanyl-D-alanine (D-Ala-D-Ala) terminus of the peptidoglycan precursors. This attachment prevents their inclusion in the expanding cell wall, interrupting cell wall growth and cross-linking, resulting in cell death (Shao et al., 2025).

Daptomycin: Being a cyclic lipopeptide, daptomycin exhibits a unique mechanism of action. Presence of calcium ions leads to binding with the bacterial cell membrane, resulting in a swift depolarization of the membrane potential. This disturbance impacts membrane activity, hindering the synthesis of proteins, DNA, and RNA, leading to swift bacterial cell death (Shao et al., 2025).

Linezolid and Tedizolid: These antibiotics of the oxazolidinone class inhibit protein synthesis in bacteria. They attach to the 23S ribosomal RNA of the 50S ribosomal subunit. Binding of this prevents the creation of the functional 70S initiation complex, which is essential for the translation process (Han et al., 2025).

Clindamycin: This antibiotic from the lincosamide class inhibits protein synthesis by attaching to the 50S ribosomal subunit (Murphy & McKay, 2015). This effectively prevents the dissociation of peptidyl tRNA from the ribosome (Armillei et al., 2024; Lin et al., 2018).

Rifampin: This drug blocks bacterial RNA synthesis by binding to the beta subunit of DNA dependent RNA polymerase, stopping the transcription process. It is often used alongside other drugs to treat biofilm-associated infections, such as those related to prosthetic joints, due to its ability to penetrate biofilms (Shao et al., 2025).

Fluoroquinolones (e.g., Ciprofloxacin): These agents block bacterial DNA replication by targeting and interfering with DNA gyrase and topoisomerase IV enzymes (Aldred et al., 2014).

3.2 Side effects

MRSA and VRSA: The widespread use of methicillin led to the quick increase of Methicillin Resistant *S. aureus* (MRSA). This limits the use of all beta-lactam antibiotics. Similarly, the growing use of vancomycin has resulted in the emergence of Vancomycin-Intermediate *S. aureus* (VISA) and Vancomycin Resistant *S. aureus* (VRSA). This complicates treatment options even more (Tarai et al., 2013).

Inducible Clindamycin Resistance: Some strains of Staphylococcus can develop inducible resistance to clindamycin. Testing, like the D-test, is necessary before use to ensure it will be effective (Prabhu et al., 2011).

Rapid Resistance to Rifampin: Rifampin should never be used alone because *S. aureus* quickly develops resistance to it. It must be combined with other antibiotics, especially in cases involving biofilm-related infections (Zimmerli & Sendi, 2019).

Linezolid Resistance: Although it is less common than MRSA, resistance to linezolid can develop during extended treatment. This primarily happens through mutations in the 23S rRNA gene (Besier et al., 2008).

3.3 Drug Toxicities and Side Effects

Numerous effective antibiotics are associated with the possibility of significant side effects. These risks may restrict their application in specific patients or necessitate close supervision.

Vancomycin Adverse Effects: Vancomycin may cause renal impairment and auditory loss, particularly when administered in large quantities or to individuals with pre-existing kidney

issues. It frequently results in "Red Man Syndrome," a response triggered by histamine release when administered too rapidly (Grabie et al., 2023).

Linezolid Adverse Reactions: Prolonged use of linezolid (exceeding 14-28 days) may lead to significant side effects. These consist of bone marrow suppression, resulting in low blood counts, peripheral neuropathy, and eyesight issues. It is additionally a mild MAO inhibitor and could interact with certain foods and drugs (Yin et al., 2025).

Daptomycin Toxicity: Daptomycin may cause muscle soreness and fatigue alongside muscle deterioration. This necessitates consistent observation of creatinine phosphokinase (CPK) levels (Berg et al., 2025).

Beta-lactam Adverse Reactions: Although these medications are usually well-tolerated, they have the potential to elicit allergic responses, varying from mild skin rashes to severe anaphylactic reactions. They may also result in digestive issues or renal complications in certain situations (Comte et al., 2024).

3.4 General Limitations of Anti-Staphylococcal Drugs

Antibiotic Resistance: The primary limitation is the Staphylococcus bacterium's remarkable capacity to gain resistance to almost all existing antibiotics. The emergence and dissemination of MRSA illustrate this problem (Fuda, Fisher, & Mobashery, 2005).

Biofilm Development: *S. aureus* frequently conceals itself in biofilms, which consist of clusters of bacteria encased in a protective matrix. Biofilms serve as a barrier and can harbor antibiotic-tolerant "persister" cells. This complicates the treatment of infections such as osteomyelitis or those associated with indwelling devices when using standard antibiotic dosages alone. Surgical intervention is often necessary (Gimza & Cassat, 2021).

Adverse Effects and Toxicity: Numerous potent anti-MRSA medications have considerable side effects, restricting their application, especially for extended therapy.

Effect on Microbiome: Broad-spectrum antibiotics can disturb the body's bacteria balance, resulting in problems like secondary infections, including Clostridioides difficile-related diarrhea (Yang et al., 2021).

Chapter 4

Previous molecular docking studies targeting staphylococcus

4.1 Article 1: "Molecular docking-based screening of methicillin-resistant Staphylococcus aureus FEM proteins with FDA-approved drugs"

This study by Akkiraju et al. (2023) uses computational methods to identify existing FDA approved drugs that may inhibit FEM proteins FemX FemB and FemC in methicillin resistant Staphylococcus aureus. These proteins are essential for building the bacterial cell wall and are not found in humans, which makes them strong antibacterial targets.

The researchers focused on FemB due to the lack of known inhibitors, while also analysing FemX and FemC. A structural model of FemB was generated using I TASSER, while published crystal structures were used for FemX and FemC. Active binding regions were predicted to guide docking studies.

A library of one thousand five hundred and thirty FDA approved compounds was screened using molecular docking and tunnel based simulations. High scoring compounds were expanded through similarity searches, and their interactions were examined in detail. Drug related properties were also predicted to assess suitability.

The results identified lumacaftor related compounds as strong binders to FemX, glycocholic acid related compounds for FemC, and hydroxyhippurate and procodazole related compounds for FemB. These findings suggest that drug repurposing may offer a practical route to developing new treatments against resistant Staphylococcus aureus.

Table 4: Computational predicted binding affinity between specific bacterial proteins and potential drug candidates

Protein	Top Hit (PubChem ID)	MolDock Score	Key Interactions
FemX	Lumacaftor-similar (90080139)	-137.66	Pi-sulfur (Tyr320), H-bonds
FemC	Glycocholic acid-similar (90473176)	-110.09	Alkyl, H-bonds
FemB	3-Hydroxyhippurate-similar (150666978)	-84.67	Pi-pi (Trp117), alkyl (Leu109)

Implications: These hits offer a foundation for novel antimicrobials, potentially enhancing β-lactam efficacy against MRSA by disrupting peptidoglycan crosslinking. Further in vitro validation and analog optimization are recommended, funded by DST-SERB.

4.2 Article 2 "Exploring the Staphylococcus aureus Gyrase Complex and Human Topoisomerase: Potential Target for Molecular Docking and Biological Studies with Substituted Polychloroaniline"

This study by Tambuwala et al., (2023),investigates three substituted polychloroanilines, PoClA, PmClA, and PomClA, for their antibacterial activity. The emphasis was on their capacity to harm bacterial DNA and attach to essential enzymes involved in DNA replication, such as Staphylococcus aureus gyrase and human topoisomerase III beta. Molecular docking and experimental tests were employed to assess their effectiveness.

The polymers were produced via chemical oxidation and subsequently analyzed using structural and imaging methods. X-ray diffraction revealed organized polymer chains, while UV-visible and FTIR analyses verified anticipated electronic transitions and bonding

configurations. Scanning electron microscopy displayed unique surface morphologies, as PmClA and PomClA exhibited layered structures, while PoClA created agglomerated chains.

Docking simulations indicated that PmClA exhibited the highest binding affinity for both target enzymes. It established strong hydrogen bonding and hydrophobic interactions in the active sites, surpassing the other two polymers. PoClA showed moderate binding, while PomClA displayed weaker interactions overall.

DNA cleavage experiments using E. coli genomic DNA revealed a different pattern. PoClA and PomClA caused clear dose dependent DNA damage, while PmClA showed little nuclease activity. This suggests that the ortho and mixed polymers act directly on DNA, while PmClA primarily interferes with enzyme function.

Overall, the findings indicate that PmClA is a strong candidate for targeting bacterial topoisomerases in Staphylococcus aureus, while PoClA and PomClA may inhibit bacterial growth through DNA cleavage. The study supports further laboratory validation of these polymers as potential antibacterial agents.

4.3 Article 3 "In silico drug design for Staphylococcus aureus and development of host-pathogen interaction network"

Wadapurkar et al. (2018) describe an in silico drug design approach to combat *Staphylococcus aureus* infections by targeting bacterial virulence rather than viability. The study builds a host pathogen interaction framework to identify how *S. aureus* proteins interact with human host factors, addressing antibiotic resistance concerns, particularly in MRSA.

A host pathogen protein interaction network was generated using STRING database data and analysed in Cytoscape. Network topology revealed highly connected virulence related bacterial hubs such as ClfA and IsdB, which play key roles in adhesion and iron acquisition, marking them as priority therapeutic targets.

Molecular docking was performed using AutoDock4 against selected virulence enzymes, including sortase A. Phytochemicals and small molecules were screened using grid based flexible docking to optimise ligand binding at active sites.

Several compounds demonstrated strong binding affinities below minus eight kcal per mol and showed favourable in silico ADMET profiles, indicating drug like properties. The integrated network and docking analysis identified over fifty critical host pathogen interactions, supporting anti virulence strategies over traditional antibiotics. The authors recommend in vitro validation to confirm these computational findings and advance antimicrobial discovery.

4.4 Article 4 "Molecular Docking and Antibacterial Activity of Campesterol Derivatives Against Staphylococcus aureus, Escherichia coli and Pseudomonas aeruginosa Multi-resistant Strains"

This research by De Morais Oliveira-Tintino et al., (2024) examined how campesterol, a sterol sourced from plants, and its altered variants might enhance the efficacy of antibiotics against bacteria resistant to multiple drugs. Released in Chemistry & Biodiversity in 2025 by De Morais Oliveira-Tintino and associates, the study examined both laboratory experiments and computer simulations to grasp how these compounds function.

Scientists evaluated campesterol along with ten of its derivatives against strains of Staphylococcus aureus, Escherichia coli, and Pseudomonas aeruginosa. When paired with antibiotics such as norfloxacin or chloramphenicol, the compounds reduced the minimum concentrations required to inhibit bacterial growth (MICs). Certain derivatives, particularly those modified with acetyl or benzoyl groups, were notably potent, decreasing MICs by as much as eightfold by disrupting bacterial efflux pumps, the proteins that bacteria rely on to expel antibiotics.

Computer docking studies demonstrated the interactions of these compounds with efflux pumps like MepA in *S. aureus* and AcrB in E. coli. Crucial interactions such as hydrogen bonds and hydrophobic contacts involving amino acids like Phe610 and Gln176 clarify their efficiency. The leading derivatives displayed binding energies lower than –8 kcal/mol, signifying a robust, non-competitive inhibition.

The findings indicate that campesterol derivatives may act as beneficial allies to current antibiotics, particularly against challenging Gram-positive bacteria such as MRSA. The integration of laboratory experiments and computational forecasts supports the need for additional research, such as pharmacokinetics, prior to testing these compounds in clinical environments.

Chapter 5

Molecular docking results

To compare phytochemicals in docking, I used the 3 reference ligands of the 2W9S receptor which are NADPH dihydro-nicotinamide-adenine-dinucleotide phosphate [ndp], trimethoprim [top], glycerol [gol]. I have used 2 distinct ligands of the modified 2W9S receptor separately, termed as Ligand 1 and Ligand 2.

Table 5: Ligand 1 molecular docking the values of GOL, NDP, TOP

Ligand	Binding affinity (kcal/mol)
GOL	-3.5
NDP	-8.4
TOP	-7.9

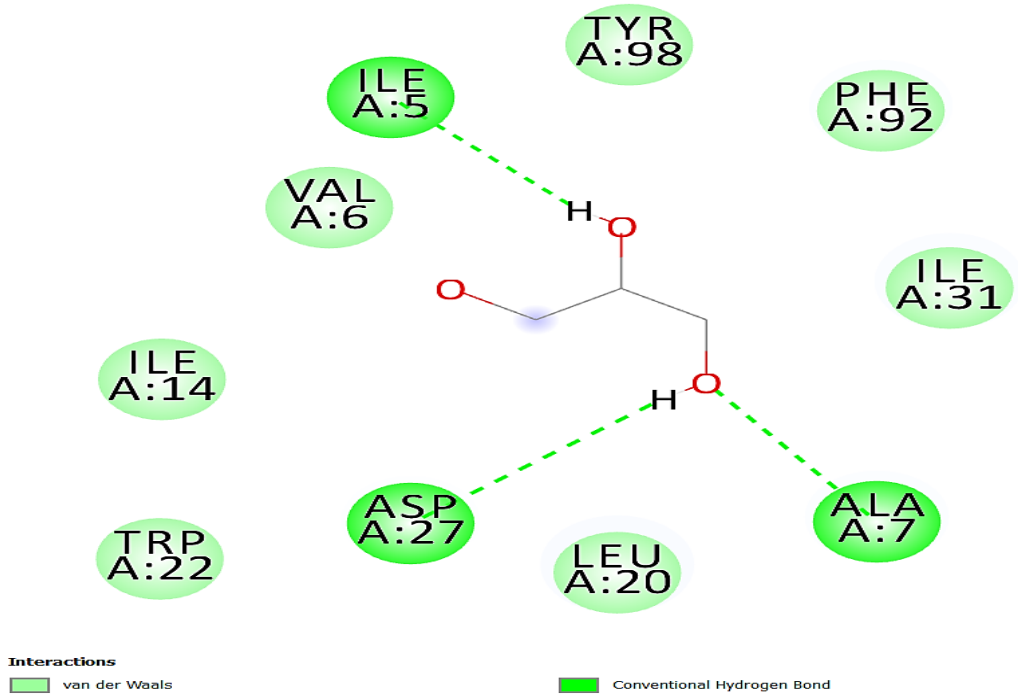

Figure 7: 2D Interaction Diagram of Glycerol (GOL) docked within the active site of S1 DHFR (PDB: 2W9S)

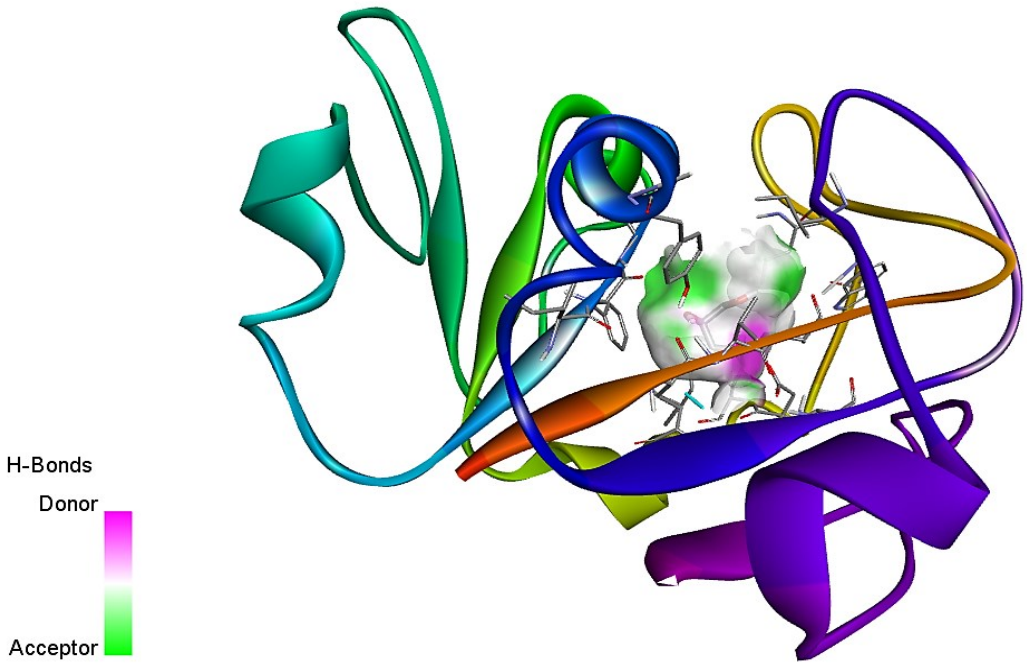

Figure 8: 3D visualization of the docking pose of Glycerol (GOL) within the active site of the S1 DHFR variant (PDB: 2W9S)

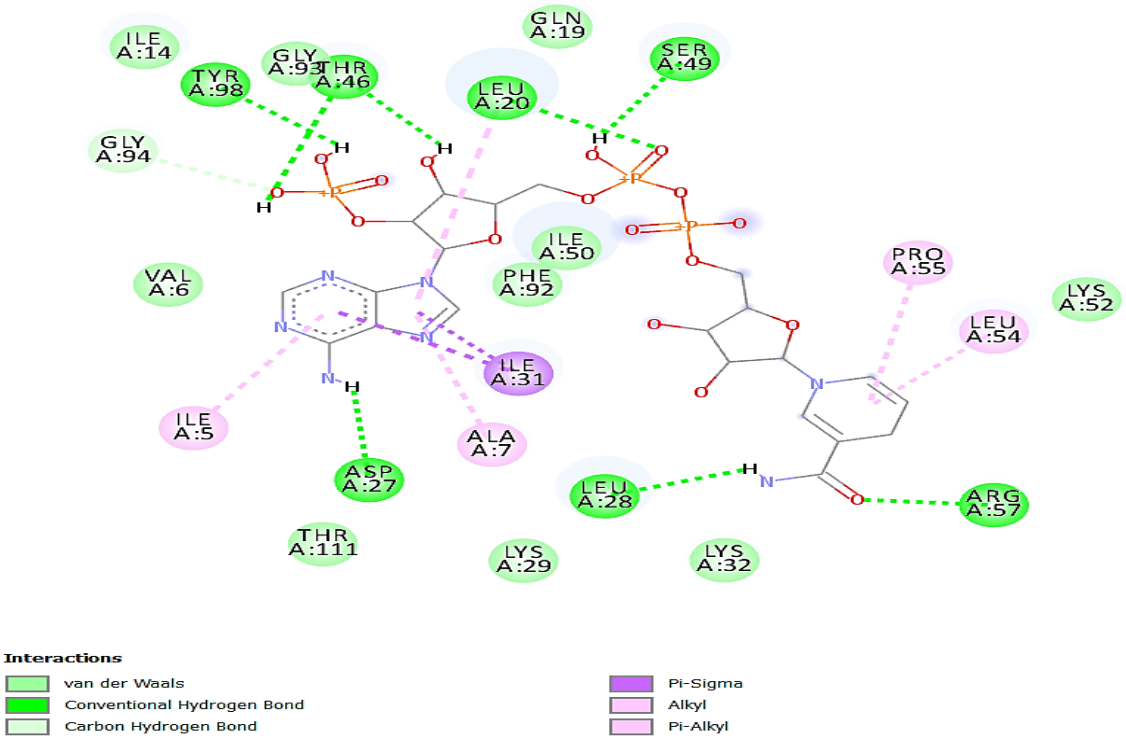

Figure 9: 2D interaction map of Trimethoprim (TOP) in the active site of S1 DHFR (PDB: 2W9S) showing reduced binding stability

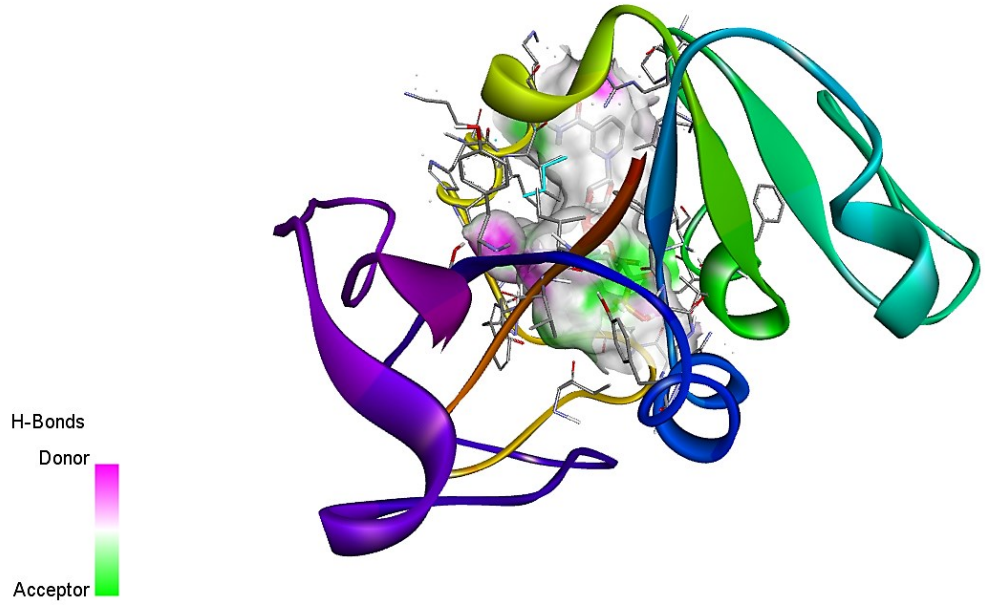

Figure 10: 3D visualization of the clinical inhibitor Trimethoprim (TOP) docked within the widened binding pocket of the 2W9S variant

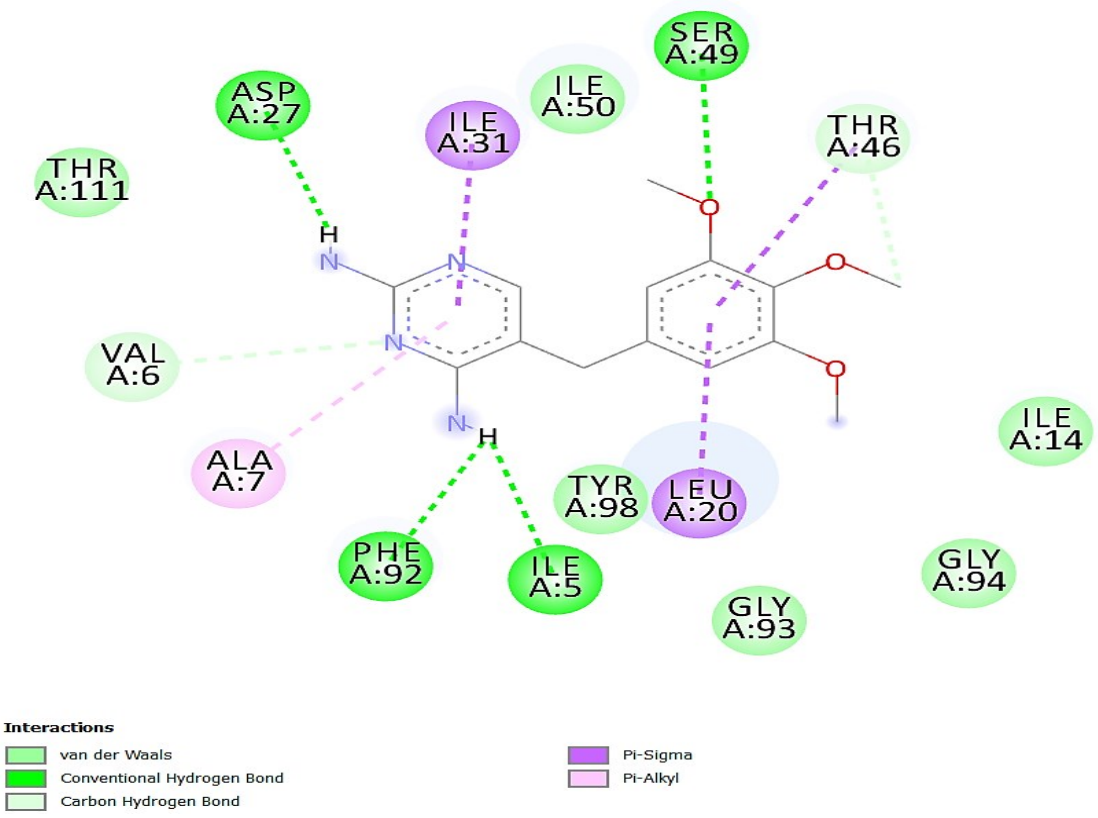

Figure 11: 2D protein-ligand interaction diagram of the natural cofactor NADPH (NDP) within the 2W9S receptor.

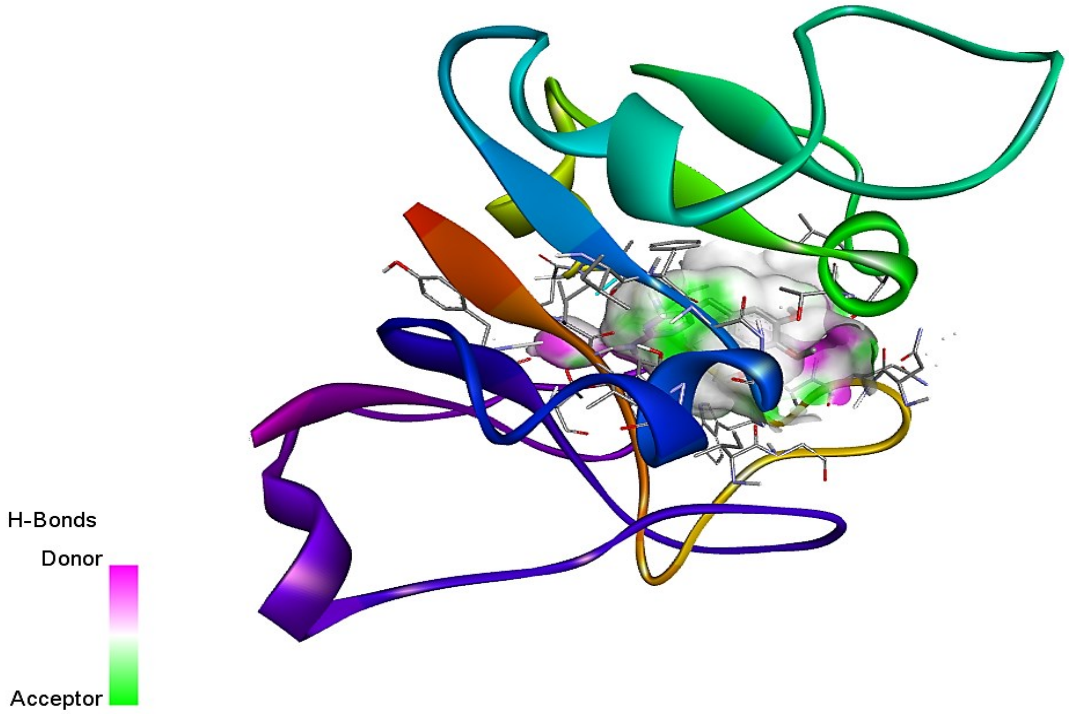

Figure 12: 3D representation of the NADPH (NDP) binding pose, demonstrating high-affinity structural conservation in the S1 DHFR variant

The conformers found from the Jahangirnagar University campus flora showed varied results depending on the conformer, but the most promising ones are:

Table 6: Ligand 1 molecular docking the values of Jahangirnagar University campus flora

Ligand	Binding affinity (kcal/mol)
Rutin-Conformer3D_COMPOUND_CID_5280805	-9.5
Neferine-Conformer3D_COMPOUND_CID_159654	-9.2
Anthocyanins-Conformer3D_COMPOUND_CID_145858	-9.1
Rosmarinic-acid-Conformer3D_COMPOUND_CID_5281792	-9.0

For Ligand 2 molecular docking the values are:

Table 7: Ligand 2 molecular docking the values of GOL, NDP, TOP

Ligand	Binding affinity (kcal/mol)
GOL	-3.8
NDP	-10.3
TOP	-7.7

The conformers found from the Jahangirnagar University campus flora showed varied results depending on the conformer, but the most promising ones are:

Table 8: Ligand 2 molecular docking the values of Jahangirnagar University campus flora

Ligand	Binding affinity (kcal/mol)
Alpha-tocopherol-Conformer3D_COMPOUND_CID_86472	-8.7
Myricetin-Conformer3D_COMPOUND_CID_5281672	-8.7
Neochlorogenic-acid-Conformer3D_COMPOUND_CID_5280633	-8.8
Rosmarinic-acid-Conformer3D_COMPOUND_CID_5281792	-8.9

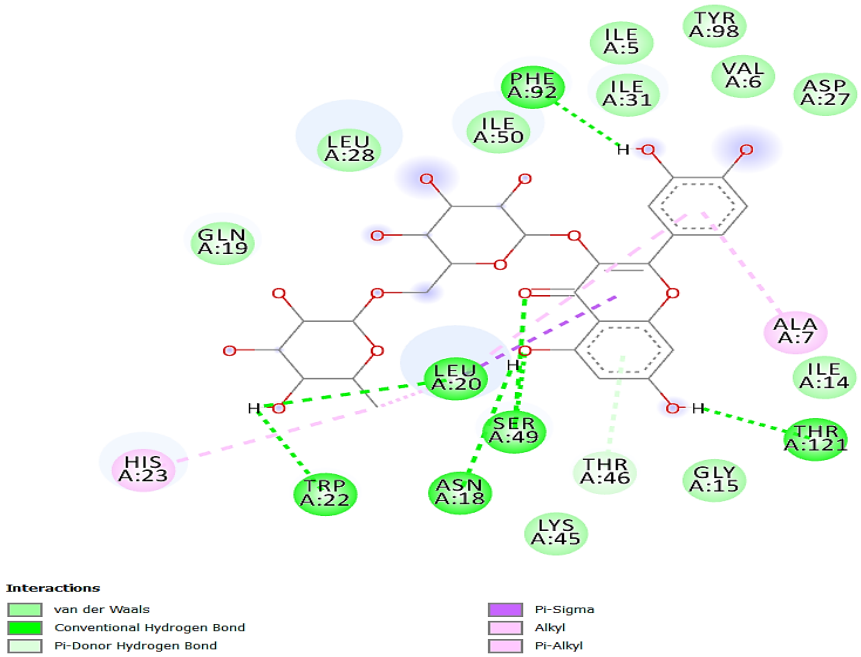

Figure 13: 2D protein-ligand interaction map of Rutin (CID 5280805) docked with S1 DHFR (PDB: 2W9S), demonstrating a superior binding affinity

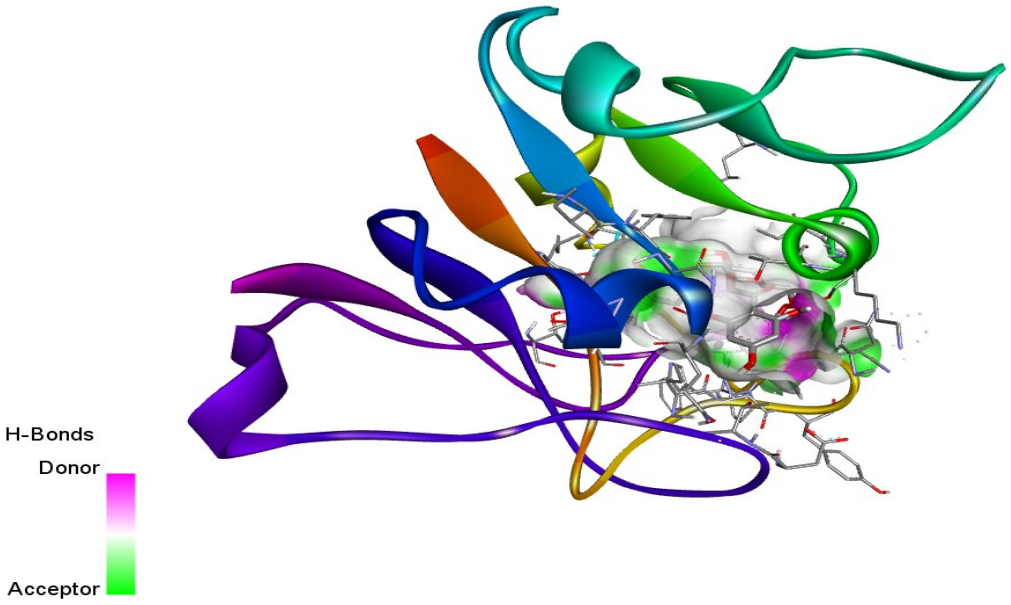

Figure 14: 3D surface representation of Rutin within the 2W9S active site, illustrating extensive pocket occupancy and hydrogen bond donor/acceptor complementarity

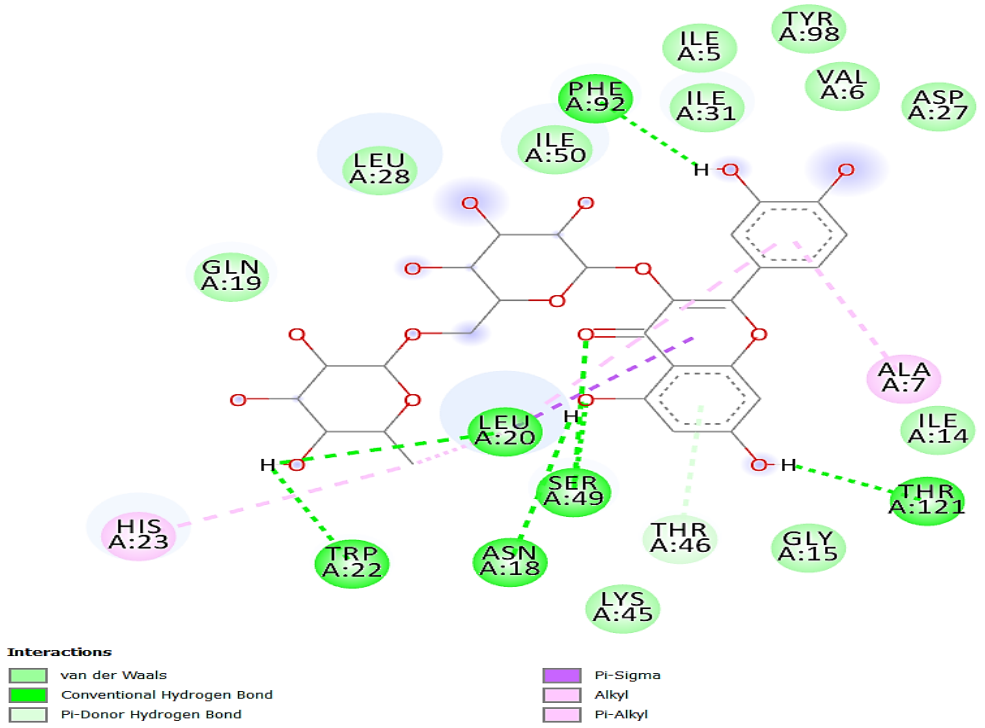

Figure 15: 2D protein-ligand interaction map of alpha-tocopherol (CID 86472) docked within the S1 DHFR receptor (PDB: 2W9S)

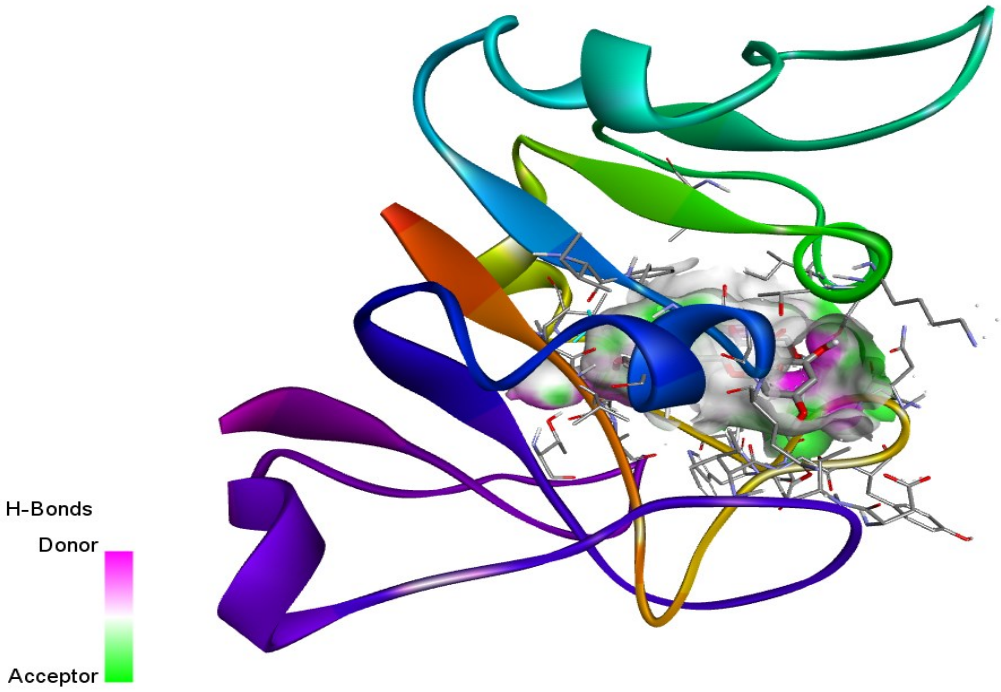

Figure 16. 3D visualization of the docking pose for alpha-tocopherol (CID 86472) in the active site of S1 DHFR, illustrating its orientation within the binding cavity

Chapter 6

Discussion

6.1 Validation of the Model

Docking scores of the reference ligands such as Trimethoprim (TOP), NADPH (NDP), and glycerol (GOL) correlate well with the already known biochemical properties of S1 DHFR mutant. It is noteworthy that the binding of Trimethoprim with S1 DHFR mutant, with a score of -7.7 to -7.9 kcal/mol, is somewhat weaker than its binding with NADPH -8.4 to -10.3 kcal/mol. This finding is consistent with the previously reported drug-binding affinity reduction, which was noted by Heaslet et al..

6.2 Identification of Superior Candidates (Ligand 1 Analysis)

In the Ligand 1 simulation, several phytochemicals significantly outperformed the standard antibiotic, Trimethoprim (-7.9 kcal/mol).

- Rutin (-9.5 kcal/mol) and Neferine (-9.2 kcal/mol) emerged as the most promising hits.
- The fact that these molecules show a more negative binding energy in other words higher affinity suggests that they may successfully navigate the widened active site and displace M20 loop of the S1 variant better than the original diaminopyrimidine scaffold of Trimethoprim.

6.3 Stability and Consistency (Ligand 2 Analysis)

The Ligand 2 simulation identified a different set of high-affinity compounds, specifically Rosmarinic acid (-8.9 kcal/mol) and Neochlorogenic acid (-8.8 kcal/mol).

Notably, Rosmarinic acid appeared as a top performer in both experiments (-9.0 and -8.9 kcal/mol), indicating high stability and consistent binding across different receptor modifications. This suggests a robust interaction pattern with the S1 active site.

6.4 Comparison with Standard Antibiotic (TOP)

In both docking scenarios, the top phytochemicals (Rutin, Neferine, Anthocyanins, and Rosmarinic acid) achieved binding energies considerably lower than Trimethoprim's average of -7.8 kcal/mol. This suggests that the phytochemical library from the Jahangirnagar University campus flora (Khan, Sultana, Hossain, Shetu, & Rahim, 2021) contains scaffolds that can potentially form stronger non-covalent interactions (such as hydrogen bonding or pi-stacking) with the altered S1 DHFR residue landscape.

6.5 Summary

The virtual screening identifies Rutin, Neferine, and Rosmarinic acid as potential hit compounds for the development of next-generation DHFR inhibitors. These molecules demonstrate the resistance-breaking potential required to inhibit the S1 variant of *S. aureus*. Further studies, such as Molecular Dynamics (MD) simulations and *in vitro* enzymatic assays are needed to validate these computational hits as viable candidates for treating TMP-resistant MRSA.

Chapter 7

Conclusion and Future Direction

This research was able to overcome the problem of resistance in *S. aureus* by focusing on the plasmid-encoded S1 DHFR variant (PDB 2W9S). With the help of structural resistance maps generated by Heaslet et al., this study has surpassed the conventional approach of diaminopyrimidines in the development of novel inhibitors from phytochemicals.

The baseline docking of reference ligands validated the computational model, showing that Trimethoprim (TOP) possesses a significantly lower affinity (avg. -7.8 kcal/mol) for the S1 variant than its natural cofactor, NADPH (avg. -9.35 kcal/mol). This disparity confirms the structural reality of the S1 variant that is a widened active site and a displaced M20 loop that effectively rejects standard antibiotics.

The high-throughput virtual screening of the some of the Jahangirnagar University campus flora identified several high-potential hits. Specifically:

- Rutin (-9.5 kcal/mol) and Neferine (-9.2 kcal/mol) emerged as the most potent candidates, likely due to their larger molecular volumes and ability to form extensive hydrogen-bonding networks that bridge the widened active site.
- Rosmarinic acid (-8.95 kcal/mol) demonstrated remarkable stability and reproducibility across multiple docking setups, identifying it as a highly reliable hit compound.

Ultimately, these results suggest that phytochemicals, particularly those with polyphenolic and alkaloid scaffolds possess the steric and electronic characteristics necessary to overcome the 1270-fold loss in binding affinity typically seen in S1-mediated resistance (Heaslet et al., 2009).

While this computational study provides a robust computational foundation, it serves as the first stage in a larger drug discovery pipeline. The following areas are proposed for future investigation:

1. Molecular Dynamics (MD) Simulations

Docking gives an insight into the binding potential of the complex under study in the static condition. Further investigation may be conducted using MD simulations for 100-200 ns to assess the stability of the complexes (e.g., Rutin-2W9S) in a dynamic aqueous condition. This will determine whether the screened phytochemicals continue to retain their binding potential when the loop is dynamic (Hollingsworth & Dror, 2018).

2. ADMET and Pharmacokinetic Profiling

To move toward clinical application, the top leads must be screened for Absorption, Distribution, Metabolism, Excretion, and Toxicity (ADMET). Evaluating the drug-likeness (Lipinski's Rule of Five) and blood-brain barrier permeability of compounds like Neferine will determine their viability as systemic antibiotics (Lipinski et al., 2001).

3. *In Vitro* Enzymatic Assays

Computational "hits" must be validated through laboratory experiments. Measuring the IC50 (half-maximal inhibitory concentration) of Rutin and Rosmarinic acid against purified S1 DHFR enzyme would provide the necessary empirical proof needed to confirm their "resistance-breaking" potential (Heaslet et al., 2009).

4. Derivative Synthesis and SAR Studies

Medicinal chemists can conduct structure-activity relationship (SAR) analysis based on the phytochemicals identified above as the parent scaffolds. Modification of certain functional groups on the scaffold structures of Rutin and Neferine is likely to increase their compatibility

with the enlarged pocket S1, thereby may give rise to a totally new generation of antibiotics against MRSA (Frey et al., 2010).

In medicine development, we are seeing the clinical standard Trimethoprim fail more frequently against resistant MRSA. This study shows us exactly why: the bacteria have structurally outsmarted the drug. By integrating high-tech virtual screening with the unique chemical profiles of natural phytochemicals, we have identified a new path forward. By shifting our focus toward these plant-based compounds, we aren't just finding alternatives; we are discovering high-potential hit candidates that can bypass the structural barriers of resistance. This work moves us closer to a future where we have a diverse and effective toolkit to treat even the most stubborn infections, ensuring that we stay one step ahead in the race against antimicrobial resistance.

References

Akkiraju, A. G., Badugu, A., Das, A., & Sagurthi, S. R. (2023). Molecular docking-based screening of methicillin-resistant *Staphylococcus aureus* FEM proteins with FDA-approved drugs. *Bioinformation*, *19*(10), 1035–1041. https://doi.org/10.6026/973206300191035

Aldred, K. J., Kerns, R. J., & Osheroff, N. (2014). Mechanism of quinolone action and resistance. *Biochemistry*, *53*(10), 1565–1574. https://doi.org/10.1021/bi5000564

Armillei, M. K., Lomakin, I. B., Del Rosso, J. Q., Grada, A., & Bunick, C. G. (2024). Scientific rationale and clinical basis for clindamycin use in the treatment of dermatologic disease. *Antibiotics*, *13*(3), 270. https://doi.org/10.3390/antibiotics1303270

Berg, D., Binkley, A., Maguire, C., Norris, A., & Athans, V. (2025). Daptomycin-induced creatine phosphokinase elevations among patients requiring outpatient parenteral antimicrobial therapy. *Open Forum Infectious Diseases*, *12*(Supplement_1), ofae631.2038. https://doi.org/10.1093/ofid/ofae631.2038

Besier, S., Ludwig, A., Zander, J., Brade, V., & Wichelhaus, T. A. (2008). Linezolid resistance in *Staphylococcus aureus*: Gene dosage effect, stability, fitness costs, and cross-resistances. *Antimicrobial Agents and Chemotherapy*, *52*(4), 1570–1572. https://doi.org/10.1128/AAC.01098-07

Bozdogan, B., Bosgelmez-Tinaz, G., Kenar, L., Yalcin, A. N., Demir, H., & Onlen, Y. (2012). Ultrastructure of a novel bacterial form located in *Staphylococcus* catheter biofilms. *Journal of Histochemistry & Cytochemistry*, *60*(10), 731–738. https://doi.org/10.1369/0022155412457573

Chambers, H. F., & DeLeo, F. R. (2009). Waves of resistance: *Staphylococcus aureus* in the antibiotic era. *Nature Reviews Microbiology*, *7*(9), 629–641. https://doi.org/10.1038/nrmicro2200

Cheung, G. Y. C., Bae, J. S., & Otto, M. (2021). Pathogenicity and virulence of *Staphylococcus aureus*. *Virulence*, *12*(1), 547–569. https://doi.org/10.1080/21505594.2021.1878688

Comte, D., Iuliano, S., Senn, L., & et al. (2024). *Management of beta-lactam antibiotics allergy: A real-life study*. Authorea. https://doi.org/10.22541/au.170669308.82543527/v1

De Morais Oliveira-Tintino, S. R., Genú de Oliveira, M., Rocha, J. E., Silva, J. L., de Freitas, T. S., Coutinho, H. D. M., & Tintino, S. R. (2024). Molecular docking and antibacterial activity of campesterol derivatives against *Staphylococcus aureus*, *Escherichia coli* and *Pseudomonas aeruginosa* multiresistant strains. *Chemistry & Biodiversity*. Advance online publication. https://doi.org/10.1002/cbdv.202401073

Effelsberg, N., Stegger, M., Peitzmann, L., Altinok, O., Coombs, G. W., Pichon, B., Kearns, A., Randad, P. R., Heaney, C. D., Bletz, S., Schaumburg, F., & Mellmann, A. (2021). Distribution and evolution of the *dfrG* gene in *Staphylococcus aureus*. *Journal of Clinical Microbiology*, *59*(3), e02198-20. https://doi.org/10.1128/jcm.02198-20

Effelsberg, N., Stegger, M. P., Peitzmann, L., Altınök, O., Coombs, G. W., Pichon, B., Kearns, A., Randad, P. R., Heaney, C. D., Bletz, S., Schaumburg, F., & Mellmann, A. (2021). Global epidemiology and evolutionary history of *Staphylococcus aureus* ST45. *Journal of Clinical Microbiology*, *59*(1), e02198-20. https://doi.org/10.1128/jcm.02198-20

Encyclopaedia Britannica. (2025, October 13). *Staphylococcus*. Britannica. https://www.britannica.com/science/Staphylococcus

Foster, T. (1996). Staphylococcus. In S. Baron (Ed.), *Medical Microbiology* (4th ed.). University of Texas Medical Branch at Galveston. https://www.ncbi.nlm.nih.gov/books/NBK8448

Frey, K. M., Lombardo, M. N., Wright, D. L., & Anderson, A. C. (2010). Towards the understanding of resistance mechanisms in clinically isolated trimethoprim-resistant, methicillin-resistant *Staphylococcus aureus* dihydrofolate reductase. *Journal of Structural Biology*, *170*(1), 93–97. https://doi.org/10.1016/j.jsb.2009.12.011

Fuda, C. C., Fisher, J. F., & Mobashery, S. (2005). Beta-lactam resistance in *Staphylococcus aureus*: The adaptive resistance of a plastic genome. *Cellular and Molecular Life Sciences*, *62*(22), 2617–2633. https://doi.org/10.1007/s00018-005-5148-6

Gimza, B. D., & Cassat, J. E. (2021). Mechanisms of antibiotic failure during *Staphylococcus aureus* osteomyelitis. *Frontiers in Immunology*, *12*, 638085. https://doi.org/10.3389/fimmu.2021.638085

Gorchynski, J., & Rose, J. K. (2008). Complications of MRSA treatment: Linezolid-induced myelosuppression presenting with pancytopenia. *Western Journal of Emergency Medicine*, *9*(3), 177–178. https://pmc.ncbi.nlm.nih.gov/articles/PMC2672264/

Grabie, Y. Y., Chain, S., Xerras, M., Hong, K., & Khan, S. A. (2023). Emergence of rapid-onset ototoxicity following three doses of vancomycin: A unique case report in the context of normal renal function and therapeutic dosing. *Cureus*, *15*(11), e48647. https://doi.org/10.7759/cureus.48647

Han, T., Jia, T., & Wang, J. (2025). Diversity in adaptive evolution of methicillin-resistant *Staphylococcus aureus* clinical isolates under exposure to continuous linezolid stress in vitro. *Infection and Drug Resistance*, *18*, 819–834. https://doi.org/10.2147/idr.s493139

Hasanpour, A. H., Sepidarkish, M., Mollalo, A., Ardekani, A., Almukhtar, M., Mechaal, A., Hosseini, S. R., Bayani, M., Javanian, M., & Rostami, A. (2023). The global prevalence of methicillin-resistant *Staphylococcus aureus* colonization in residents of elderly care centers: A systematic review and meta-analysis. *Antimicrobial Resistance & Infection Control*, *12*(1), 4. https://doi.org/10.1186/s13756-023-01210-6

Heaslet, H., Harris, M., Ludtke, K., Messado, N., Sun, L., Tiarks, J., Dellas, N., Hruza, A., & Anderson, M. S. (2009). Structural and biochemical characterization of the *S. aureus* dihydrofolate reductase S1 variant: Mechanism of trimethoprim resistance. *Proteins: Structure, Function, and Bioinformatics*, *76*(4), 806–817. https://doi.org/10.1002/prot.22383

Khan, S. A., Sultana, S., Hossain, G. M., Shetu, S. S., & Rahim, M. A. (2021). Floristic composition of Jahangirnagar University Campus - A semi-natural area of Bangladesh. *Bangladesh Journal of Plant Taxonomy*, *28*(1), 27–60. https://doi.org/10.3329/bjpt.v28i1.54207

Licitra, G. (2013). Etymologia: *Staphylococcus*. *Emerging Infectious Diseases*, *19*(9), 1553. https://doi.org/10.3201/eid1909.ET1909

Lipinski, C. A., Lombardo, F., Dominy, B. W., & Feeney, P. J. (2001). Experimental and computational approaches to estimate solubility and permeability in drug discovery and development settings. *Advanced Drug Delivery Reviews*, *46*(1–3), 3–26. https://doi.org/10.1016/S0169-409X(00)00129-0

Liu, A., Garrett, S., Hong, W., & Zhang, J. (2024). *Staphylococcus aureus* infections and human intestinal microbiota. *Pathogens*, *13*(4), 276. https://doi.org/10.3390/pathogens1304276

Murphy, C. S., & McKay, G. (2015). Clindamycin. *Practical Diabetes*, *32*(6), 222–223a. https://doi.org/10.1002/pdi.1962

Prabhu, K., Rao, S., & Rao, V. (2011). Inducible clindamycin resistance in *Staphylococcus aureus* isolated from clinical samples. *Journal of Laboratory Physicians*, *3*(1), 25–27. https://doi.org/10.4103/0974-2727.78558

Rowe, S. E., Beam, J. E., & Conlon, B. P. (2021). Recalcitrant *Staphylococcus aureus* infections: Obstacles and solutions. *Infection and Immunity*, *89*(4), e00694-20. https://doi.org/10.1128/IAI.00694-20

Shao, K., Yang, Y., Gong, X., Chen, K., Liao, Z., & Ojha, S. C. (2025). Staphylococcal drug resistance: Mechanisms, therapies, and nanoparticle interventions. *Infection and Drug Resistance*, *18*, 1007–1033. https://doi.org/10.2147/IDR.S510024

Tambuwala, M. M., Kunda, N., Niaz, Z., Aljabali, A. A. A., & Mishra, V. (2023). Exploring the *Staphylococcus aureus* gyrase complex and polymeric compounds: An approach to combat antimicrobial resistance. *Cureus*, *15*(11), e49029. https://doi.org/10.7759/cureus.49029

Tania, N. E. J., Shamsuzzaman, S. M., Islam, A., Rahman, M. M., & Kubra, K. (2023). Prevalence and antibiotic resistance pattern of *Staphylococcus aureus* isolated from clinical samples: A cross-sectional study. *Bangladesh Journal of Medical Microbiology*, *17*(1), 29–33. https://doi.org/10.3329/bjmm.v17i1.68265

Tarai, B., Das, P., & Kumar, D. (2013). Recurrent challenges for clinicians: Emergence of methicillin-resistant *Staphylococcus aureus*, vancomycin resistance, and current treatment options. *Journal of Laboratory Physicians*, *5*(2), 71–78. https://doi.org/10.4103/0974-2727.119843

Touaitia, R., Mairi, A., Ibrahim, N. A., Basher, N. S., Idres, T., & Touati, A. (2025). *Staphylococcus aureus*: A review of the pathogenesis and virulence mechanisms. *Antibiotics*, *14*(5), 470. https://doi.org/10.3390/antibiotics14050470

UK Standards for Microbiology Investigations. (2020). *Identification of Staphylococcus species, Micrococcus species and Rothia species (UK SMI ID 7i4)*. Public Health England. https://www.rcpath.org/static/db5f13cb-53ca-4e9e-a0937b78b610d0ac/4dde3cf8-f775-4f31-9a351b100e2742af/uk-smi-id-7i4-identification-of-staphylococcus-species-micrococcus-species-and-rothia-species-may-2020-pdf.pdf

Vanamala, K., Tatiparti, K., Bhise, K., Sau, S., Scheetz, M. H., Rybak, M. J., Andes, D., & Iyer, A. K. (2021). Novel approaches for the treatment of methicillin-resistant *Staphylococcus aureus*: Using nanoparticles to overcome multidrug resistance. *Drug Discovery Today*, *26*(1), 31–43. https://doi.org/10.1016/j.drudis.2020.10.011

Wadapurkar, R. M., Shilpa, M. D., Katti, A. K. S., & Sulochana, M. B. (2018). In silico drug design for *Staphylococcus aureus* and development of host-pathogen interaction network. *Informatics in Medicine Unlocked*, *12*, 114–121. https://doi.org/10.1016/j.imu.2017.12.005

Yang, L., Bajinka, O., Jarju, P. O., Tan, Y., Taal, A. M., & Ozdemir, G. (2021). The varying effects of antibiotics on gut microbiota. *AMB Express*, *11*(1), 116. https://doi.org/10.1186/s13568-021-01274-w

Yin, J., Chen, X., Sun, J., Wang, Y., & Wang, K. (2025). Risk assessment of linezolid-associated neurological adverse drug reactions based on the Food and Drug Administration Adverse Event Reporting System database. *Journal of Multidisciplinary Healthcare*, *18*, 2969–2981. https://doi.org/10.2147/JMDH.S507827